PAPER

A novel hybrid multi-criteria optimization of 3D printing process using grey relational analysis (GRA) coupled with principal component analysis (PCA)

Engineering Research Express

PAPER

A novel hybrid multi-criteria optimization of 3D printing process using grey relational analysis (GRA) coupled with principal component analysis (PCA)

RECEIVED
2 November 2023

REVISED
22 January 2024

ACCEPTED FOR PUBLICATION
26 January 2024

PUBLISHED
6 February 2024

Rajeev Ranjan[1,*] **and Abhijit Saha**[2]

[1] Department of Mechanical Engineering, Dr B.C. Roy Engineering College, Durgapur, India
[2] Department of Mechanical Engineering, Haldia Institute of Technology, Haldia, India
[*] Author to whom any correspondence should be addressed.

E-mail: rajeevranjan.br@gmail.com **and** alfa.nita2010@gmail.com

Keywords: 3D printing, FDM, PLA, hybrid optimization, GRA, PCA

Abstract

Fused deposition modeling (FDM) is renowned as a prominent approach in the realm of 3D printing, where objects are built layer by layer using a heated nozzle to extrude melted materials. This research was conducted to identify the most effective FDM process variables to enhance tensile strength while simultaneously reducing surface roughness. Polylactic Acid (PLA) was chosen to fabricate test samples, showcasing the applications of 3D printing. In the course of this research, we conducted a series of 27 experiments to investigate the fundamental relationship between the parameters and the corresponding responses. The central aim of this study lies in optimizing the input variables viz. printing speed, layer thickness, and carbon deposition (C-deposition) for the technological manufacturing process of embossing parts in the context of Industry 4.0. To enhance both tensile strength and surface roughness simultaneously, a new hybrid method has been suggested. This approach integrates grey relational analysis (GRA) with principal component analysis (PCA) to determine the optimal combination of process parameters in the 3D printing process. Notably, the experiment trial exhibited the highest grey relational grade (GRG), indicating optimal process parameter settings at a printing speed of 100 mm s^{-1}, layer thickness of 0.1 mm, and C-deposition of 15 mg respectively. Additionally, mathematical models are created through response surface methodology to explore the impact of FDM parameters on the grey relational grade. The findings from this study can be utilized in various industries and applications where FDM 3D printing is employed.

1. Introduction

In today's dynamic and consumer-oriented world, there is a growing demand for flexible, fast, and dependable production technologies. Among these technologies, additive manufacturing stands out as its applications continue to expand daily [1]. Additive manufacturing (AM) encompasses a range of advanced techniques, with 3-D printing being one of them, used to create a variety of products. First introduced around 1987, additive manufacturing involves creating a 3D object layer by layer using a computer-controlled printing program [2, 3]. These cutting-edge methods allow for the production of highly intricate products while significantly reducing waste during the manufacturing process [4, 5].

One of the diverse methods within additive manufacturing is fused deposition modeling (FDM), which utilizes melted thermoplastic filaments to build structures. Its simplicity, accessibility, and adaptability have led to a resurgence in its use. Over nearly forty years of development, FDM technology has progressed to the point where it can be employed to produce reinforced composite structures with a range of materials, such as nanomaterials, ceramics [6], polymeric materials [7], and different fibers. Although commonly used with

thermoplastics like nylon [8], and polylactic acid [9], promising results have been achieved by using thermoset matrix materials [10, 11], which tend to offer higher strength.

Scientists have been investigating a range of processing variables to elucidate their impact on the characteristics of 3D-printed components fabricated using Fused Deposition Modeling (FDM). Several prior studies have delved into examining how processing parameters affect the functionality of 3D-printed parts are summarized in table 1.

The accuracy of FDM techniques poses a challenge due to the interdependence of numerous variables involved in the process. Altering one parameter can lead to significant changes in other aspects, making it difficult to predict the outcome accurately. This lack of predictability may hinder precise process control, thereby affecting the quality and cost-effectiveness of the final printed products. To keep up with the growing demand and explore new possibilities, it is crucial to delve further into 3D printing. This entails fine-tuning process parameters to enhance product quality and achieve cost efficiency [4]. Hybrid optimization techniques stand out as highly effective methods [36], This is because they harness the unique capabilities of two or more individual methods. By emphasizing these facets, we can greatly propel the future of 3D printing.

Numerous diverse hybrid approaches have been employed in recent decades to enhance the optimization of 3D printing process parameters. In a recent study, the use of GRA and fuzzy TOPSIS was explored for selecting 3D printing techniques. The results obtained from GRA were compared with those from fuzzy TOPSIS, and it was determined that SLS emerged as the most suitable process due to its exceptional performance in both dimensional accuracy and surface quality [37], In a separate investigation, researchers employed the grey-based Taguchi technique to refine the build orientation, part fill style, and slice height of FDM. This comprehensive analysis considered various response parameters, such as hardness, surface roughness, and build time, and the optimization results were further validated using a hybrid approach involving AHP and TOPSIS [38], Meanwhile, another group of researchers delved into examining the influence of gas flow rate, welding speed, and current on SS308L sample properties produced via wire arc 3D printing-cold metal transfer process. They pursued optimal process parameters through an integrated MADM approach, incorporating fuzzy MARCOS, fuzzy AHP, and analysis of means [39]. Also, a MADM technique based on VIKOR and AHP was introduced to facilitate the selection of the most appropriate process parameters for FDM. This method concurrently optimized infill percentage, printing speed, layer thickness, and zig-zag pattern for FDM [40].

Drawing from existing literature, there is much research on optimizing 3D printing process parameters using a variety of methods. Nonetheless, little is known about the optimization of FDM using a hybrid multi-objective approach. Henceforth, the unique aspect of this study lies in the optimizing method used to enhance the process parameters. This novel approach offers potential advantages for professionals in the fields of 3D printing and other rapid prototyping techniques, allowing them to apply the methodology demonstrated here to various processes. This paper employs a novel hybrid method, combining GRA with PCA, to determine the most suitable 3D printing process parameters, aiming to enhance mechanical and surface texture properties. These processing parameters include the printing speed, layer thickness, and carbon deposition (C-deposition). Each of these elements has a notable impact on establishing the robustness, longevity, and exterior characteristics of the produced items.

2. Materials and methods

Polylactic Acid (PLA) serves as a commonly used thermoplastic polymer in fused deposition modeling (FDM) technique [41]. This entirely eco-friendly substance is sourced from sustainable raw materials, like corn starch, making it environmentally friendly. Additionally, PLA is affordable and comes in various colors. The strength of PLA parts depends on numerous interconnected factors. The submicron-sized carbon particles can improve the mechanical characteristics of the 3D-printed parts [31]. In this study, the focus was on three controllable variables: printing speed, layer thickness, and C-deposition, which were carefully selected based on previous literature and the capabilities of the Ender-3 V2 FDM 3D printer. The diagram illustrating the experimental layout can be found in figure 1.

Different levels of these process parameters, as shown in table 2, were set to conduct the experimental work, and the parts were fabricated using the chosen 3D printing machine. Table 3 presents the outcomes of the experiments. Following the experiments, the average surface roughness (R_a) of all machined surfaces was assessed using Taylor Hobson's Talysurf, employing a cutoff length of 0.8 mm.

3. Hybrid optimization methodology

In this research article, a novel approach to optimizing multiple responses has been presented, which encompasses a combination of various multi-criteria decision-making techniques, namely grey relational

Table 1. Overview of the factors influencing the characteristics of 3D printed components.

Authors (year)	Process parameters	Findings/ results	Reference
Sood *et al* (2010)	Raster angle & width, layer thickness, air gap, orientation	The investigation and enhancement of the mechanical characteristics are examined through the application of RSM	[12]
Durgun *et al* (2014)	Raster angles, orientations	Proposed that the orientation has a greater impact compared to the angle of the raster on both the surface texture and mechanical characteristics	[13]
Onwubolu *et al* (2014)	Raster angle & width, layer thickness, air gap, orientation	Documented the ideal procedural conditions for enhancing tensile strength	[14]
Nunez *et al* (2015)	Layer thickness, infill density	The dimensional precision as well as surface characteristics can be influenced by altering the layer thickness and infill density	[15]
Baich *et al* (2015)	Infill density	A greater infill density not only boosts strength but also influences production expenses	[16]
Wu *et al* (2015)	Raster angle, layer thickness	Best mechanical characteristics were observed when the layer thickness was set to 300 μm and the raster angle was 0°.	[17]
Behzadnasab *et al* (2016)	Nozzle temperature	The nozzle temperature setting determines the quality of the printed components.	[18]
Christiyan *et al* (2016)	Printing speed, layer thickness	Proposed that reducing the printing speed and minimizing the layer thickness could enhance the material's mechanical characteristics.	[19]
Dawoud *et al* (2016)	Raster angle, air gap	Proposed by carefully choosing FDM parameters, it was possible to achieve mechanical characteristics	[20]
Chacón *et al* (2017)	Layer thickness, feed rate, orientation	Determined that the upright position led to the least favorable mechanical outcome, while the edge and flat orientations yielded the greatest strength and stiffness.	[21]
Deng *et al* (2018)	Filling density, layer thickness, printing temperature, printing speed	Best tensile characteristics when printed at filling density 40%, layer thickness 0.2mm, speed 60mm s^{-1} at 370°C temperature	[22]
Khatwani *et al* (2019)	Part bed temperature, layer thickness, nozzle diameter	Tensile and flexural strength improved with higher part bed temperature but showed opposite trends with layer thickness and nozzle diameter changes.	[23]
Yadav *et al* (2020)	Infill density, printing temperature	The GA-ANN improved tensile strength by 4.54%, confirmed through experimental validation.	[24]
Selvam *et al* (2020)	Printing speed, printing temperature, layer thickness	Used spline interlock suture in CF-PLA enhances 3D-printed strength versus pure PLA, optimized with PSO	[25]
Kafshgar *et al* (2021)	Printing temperature, layer thickness, infill density, raster angle	Applied Taguchi optimization for best results in mechanical properties	[26]
Choudhary *et al* (2021)	Addition of bio-ceramics	Demonstrated that adding bioceramics to PLA reduced wear, COF, and enhanced mechanical characteristics.	[27]
Xu *et al* (2021)	Printing temperature, infill density, layer thickness	Alterations in nozzle temperature, layer thickness, and infill density impact flexural properties	[28]
Mani *et al* (2022)	Printing temperature, infill density, layer thickness	Taguchi Design applied to optimized Surface Roughness, Tensile, and Hardness.	[29]
Heidari-Rarani *et al* (2022)	Printing speed, infill density, layer thickness	The best settings for elasticity and tensile strength were found at 80% infill, 40mm.s^{-1} speed, and 0.1mm layer thickness in experiments	[30]
Raju *et al* (2022)	C-deposition, printing speed	Taguchi's method optimized tensile strength, toughness, and surface roughness	[31]
Maguluri *et al* (2023)	Printing speed, infill density, printing temperature	The findings highlighted that nozzle temperature impacts PLA tensile properties, followed by infill density.	[32]
Nagarjun *et al* (2023)	Addition of composites	Discovered the composite improved performance with a constant 2% filler concentration.	[33]

Table 1. (Continued.)

Authors (year)	Process parameters	Findings/ results	Reference
Beylergil *et al* (2023)	Printing speed, infill density, printing temperature, raster angle	Charpy-impact strength surges by 150% at 100% infill, 60° raster, 260 °C temp, and 30 mm.s^{-1} speed.	[34]
Yao *et al* (2023)	Printing speed, infill density, printing temperature	Tensile strength increased when temperature reached 190 °C, density was 50%, and speed was 20mm.s^{-1}.	[35]

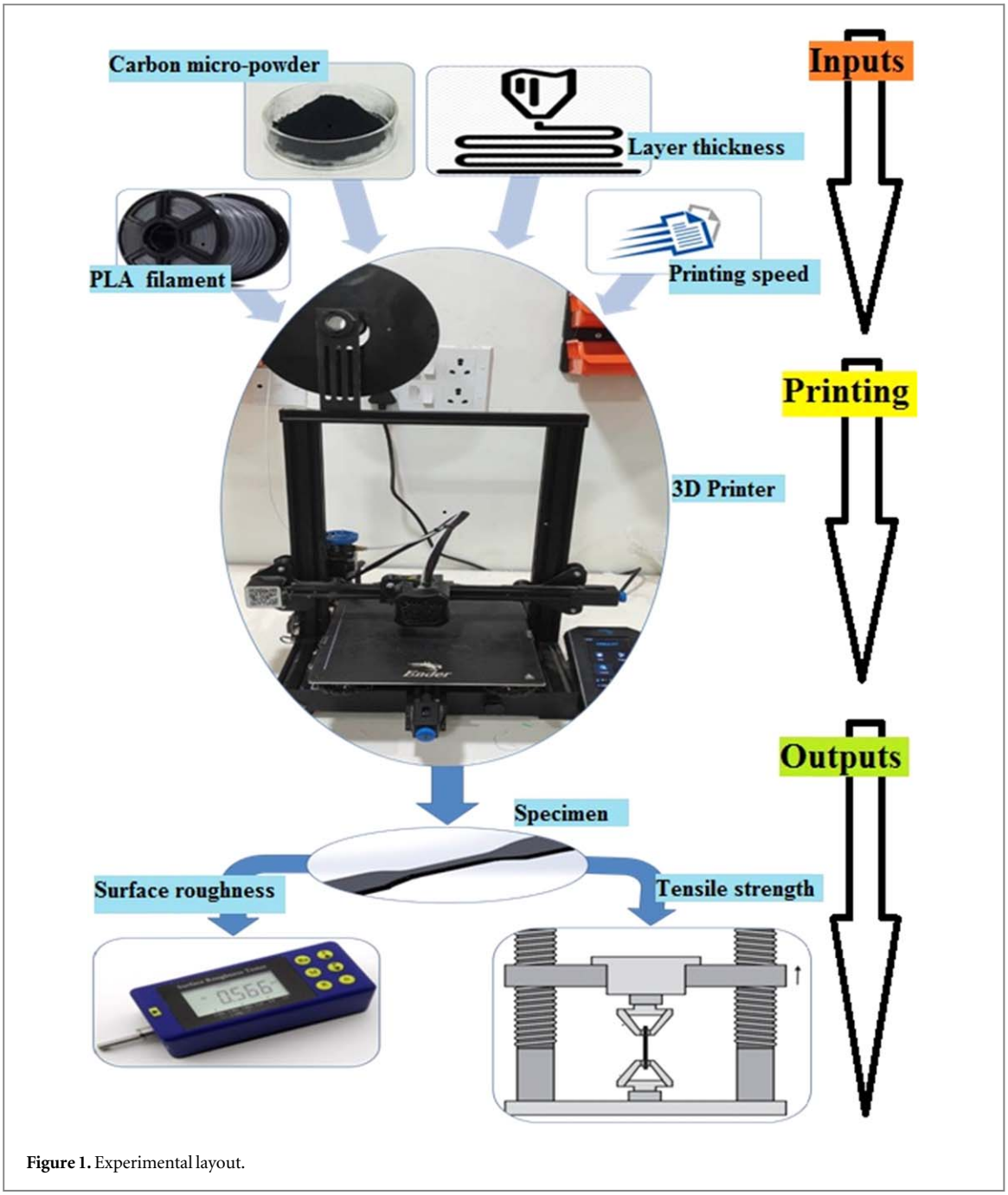

Figure 1. Experimental layout.

Table 2. Processing variables against different levels.

Sl. No.	Symbol	Parameter	Unit	1	2	3
1	A	Printing speed	mm/s	50	75	100
2	B	Layer thickness	mm	0.10	0.20	0.30
3	C	C-deposition	mg	5	10	15

analysis (GRA) and principal component analysis (PCA). The methodology consists of several well-defined steps [42–46], outlined below:

Step 1: Development of the decision matrix

The procedure begins by establishing a decision matrix and systematically enumerating both the criteria and alternatives. To evaluate how each alternative performs concerning each criterion, a distinct equation is utilized:

Table 3. Experimental observations.

Exp. No.	A	B	C	Tensile strength (MPa)	Surface roughness (microns)
1	1	1	1	7.68	0.006
2	1	1	2	8.08	0.006
3	1	1	3	7.98	0.005
4	1	2	1	8.02	0.007
5	1	2	2	8.52	0.007
6	1	2	3	8.05	0.005
7	1	3	1	7.27	0.006
8	1	3	2	8.15	0.005
9	1	3	3	7.92	0.005
10	2	1	1	8.74	0.007
11	2	1	2	8.98	0.005
12	2	1	3	8.69	0.005
13	2	2	1	9.02	0.005
14	2	2	2	7.88	0.006
15	2	2	3	8.85	0.005
16	2	3	1	8.88	0.008
17	2	3	2	9.15	0.005
18	2	3	3	9.11	0.005
19	3	1	1	8.18	0.007
20	3	1	2	8.52	0.006
21	3	1	3	10.05	0.004
22	3	2	1	8.22	0.007
23	3	2	2	8.65	0.005
24	3	2	3	8.06	0.005
25	3	3	1	7.64	0.007
26	3	3	2	8.94	0.006
27	3	3	3	8.42	0.005

$$D_{ij} = \begin{bmatrix} x_{11} & x_{12} & \ldots\ldots & x_{1n} \\ x_{21} & x_{22} & \ldots\ldots & x_{2n} \\ \ldots\ldots & \ldots\ldots & \ldots\ldots & \ldots\ldots \\ x_{m1} & x_{m2} & \ldots\ldots & x_{mn} \end{bmatrix} \quad (?1)$$

In the above context, D_{ij} represents the evaluation of the ith option concerning the jth set of criteria. The variable m signifies the total count of experiments, while n denotes the quantity of response parameters.

Step 2: Preparing the data

Data preprocessing plays a crucial role, especially when dealing with data series that have varying ranges and units. It becomes particularly important when there is a significant scatter range among the series or when the target directions within the sequence are dissimilar. The objective of data preprocessing is to convert the initial sequence into a similar one. Diverse approaches for preparing data exist when conducting grey relational analysis, depending on the specific characteristics of the data sequence, such as its quality or productivity

If the goal value of the initial sequence has no limit and follows the principle of 'higher is better,' normalization can be implemented in the following manner:

$$x_i^*(k) = \frac{x_i^0(k) - \min x_i^0(k)}{\max x_i^0(k) - \min x_i^0(k)} \quad (?2)$$

In cases where the original sequence exhibits a 'lower is better' characteristic, to address factors like surface texture, normalization can be achieved by employing the subsequent approach:

$$x_i^*(k) = \frac{\max x_i^0(k) - x_i^0(k)}{\max x_i^0(k) - \min x_i^0(k)} \quad (?3)$$

Conversely, when aiming to achieve a particular desired value, the initial sequence will undergo standardization commencing at:

$$x_i^*(k) = 1 - \frac{|x_i^0(k) - x_i^0|}{\max x_i^0(k) - x_i^0} \quad (4)$$

Alternatively, the initial sequence can be essentially standardized using the fundamental method of dividing each value by the first element of the sequence.

$$x_i^*(k) = \frac{x_i^0(k)}{x_i^0(1)} \tag{5}$$

For the given indices, when*i ranges* from 1 to *m* and *k* ranges from 1 to *n*, we have *m* representing the count of experimental data items, and *n* representing the count of parameters. The symbol $x_i^o(k)$ signifies the initial sequence, while $x_i^*(k)$ denotes the sequence after data preprocessing. The maximum value within $x_i^o(k)$ is denoted as max. $x_i^o(k)$, and the minimum value within $x_i^o(k)$is denoted as min. $x_i^o(k)$. Meanwhile, x_i^o represents the target value for $x_i^o(k)$.

Step 3: Assessment of Grey correlation factors

In this stage, the assessment revolves around the analysis of grey relational coefficients. When there's a solitary sequence, $x^o(k)$, functioning as the reference, and all remaining sequences are utilized for comparative purposes, this is referred to as a local measurement of grey relations. Following the completion of data preprocessing, the computation of the grey relation coefficient $\xi i(k)$ for the *k*th performance attribute in the *i*th experiment is undertaken to illustrate the correlation between the optimal and normalized outcomes. This expression can be presented as follows.

$$\xi_i(k) = \frac{\Delta_{\min} + \xi.\Delta_{\max}}{\Delta_{oi}(k) + \xi.\Delta_{\max}} \tag{6}$$

Where, $\Delta_{oi}(k)_{=}|x_0^*(k) - x_i^*(k)|$ and$\Delta_{\max} = 1.00$, $\Delta_{\min} = 0.00$

The deviation sequence, denoted as $\Delta_{oi}(k)$signifies the difference between the reference sequence $x_o{}^*(k)$ and the comparability sequence $x_i{}^*(k)$. The distinguishing coefficient, ξ, which ranges from 0 to 1, serves to identify the relationship between $x_o{}^*(k)$ and $x_i{}^*(k)$. A smaller ξi (k) value indicates a higher level of distinction. The purpose of this coefficient is to measure the extent of correlation between the two sequences. In the context of this study, a value of 0.5 has been assigned to ξ, which signifies an optimistic estimate derived from the normal distribution.

Step 4: Evaluation of the weighting of responses through principal component analysis

It involves assessing the response weights through principal component analysis (PCA) is a statistical method employed to convert a collection of potentially interrelated variables into a fresh set of variables that lack correlations. Significantly, the various responses from individuals vary, suggesting varying degrees of significance within the GRA, as determined in this research through the application of PCA.

The initial phase commences with the choice of several outcomes from n trials and m characteristics. In our particular study, the outcome parameters acquired through the computation of the Global Ranking Coefficient (GRC) constitute a multi-result array utilized to ascertain the criteria weights. The subsequent stage encompasses the assessment of the correlation coefficient derived from the GRC using the subsequent formula:

$$R_{jl} = \left[\frac{\mathrm{cov}(x_i(j),\, x_i(l))}{\sigma x_i(j) * \sigma x_i(l)} \right] \tag{7}$$

The evaluation of each response's GRC symbolized as $x_i(j)$, involves the consideration of the covariance (cov) between response variables *j* and *l*, which is represented as $x_i(l)$. Furthermore, we also factor in the standard deviation (σ) of each response variable, which is denoted as $\sigma x_i(j)$ and $\sigma x_i(l)$. Consequently, we calculate eigenvalues and their associated eigenvectors using equation (8).

$$(R - \lambda_x I_m) V_{ik} = 0 \tag{8}$$

Where λ_x eigenvalues, $\sum_{k=1}^{n} \lambda_k = n, k$ =1,2,…….n, and $V_{ik}[a_{k1,}a_{k2\ldots\ldots,}a_{km}]^T$ are the eigenvectors associated with eigenvalues.

As a result, the primary elements are derived from the equation (9)

$$Y_{mk} = \sum_{i=1}^{n} x_m(i)\, V_{ik} \tag{9}$$

The initial principal component is denoted as Y_{m1}, followed by Y_{m2} as the second component, and so forth. These components are arranged in descending order based on their variance, meaning that Y_{m1}, being the first principal component, captures the highest variance within the data.

Step 5: Assessment of the comprehensive grey relational grades

The gray relational grades (GRG) are determined by assessing the average GRC value associated with each of the process responses, as indicated by the subsequent formula:

$$\gamma_i = \frac{1}{n} \quad \sum_{j=1}^{n} \beta_j \quad \xi_i(k) \tag{10}$$

In this context, the grey relational grade γ_i indicates the degree of correlation between the reference sequence and the comparability sequence. The weights $\beta(j)$ for the process parameters are computed using the formula in

Table 4. Details calculations of the GRA-PCA Method.

Exp.No.	Grey relational generation		Deviation sequence		Grey relational coefficient			
	Tensile strength (MPa)	Surface roughness (microns)	Tensile strength (MPa)	Surface roughness (microns)	Tensile strength (MPa)	Surface roughness (microns)	Grey relational grades	Rank
1	0.15	0.50	0.85	0.50	0.37	0.50	0.217	22
2	0.29	0.50	0.71	0.50	0.41	0.50	0.228	18
3	0.26	0.75	0.74	0.25	0.40	0.67	0.267	13
4	0.27	0.25	0.73	0.75	0.41	0.40	0.202	26
5	0.45	0.25	0.55	0.75	0.48	0.40	0.219	21
6	0.28	0.75	0.72	0.25	0.41	0.67	0.269	12
7	0.00	0.50	1.00	0.50	0.33	0.50	0.208	23
8	0.32	0.75	0.68	0.25	0.42	0.67	0.272	10
9	0.23	0.75	0.77	0.25	0.39	0.67	0.265	14
10	0.53	0.25	0.47	0.75	0.51	0.40	0.229	17
11	0.62	0.75	0.38	0.25	0.57	0.67	0.308	5
12	0.51	0.75	0.49	0.25	0.51	0.67	0.293	7
13	0.63	0.75	0.37	0.25	0.57	0.67	0.310	4
14	0.22	0.50	0.78	0.50	0.39	0.50	0.223	19
15	0.57	0.75	0.43	0.25	0.54	0.67	0.301	6
16	0.58	0.00	0.42	1.00	0.54	0.33	0.219	20
17	0.68	0.75	0.32	0.25	0.61	0.67	0.318	2
18	0.66	0.75	0.34	0.25	0.60	0.67	0.316	3
19	0.33	0.25	0.67	0.75	0.43	0.40	0.207	25
20	0.45	0.50	0.55	0.50	0.48	0.50	0.244	16
21	1.00	1.00	0.00	0.00	1.00	1.00	0.500	1
22	0.34	0.25	0.66	0.75	0.43	0.40	0.208	24
23	0.50	0.75	0.50	0.25	0.50	0.67	0.291	8
24	0.28	0.75	0.72	0.25	0.41	0.67	0.269	11
25	0.13	0.25	0.87	0.75	0.37	0.40	0.191	27
26	0.60	0.50	0.40	0.50	0.56	0.50	0.264	15
27	0.41	0.75	0.59	0.25	0.46	0.67	0.282	9

equation (9). The evaluation of the best multi-response parameter design depends on the GRG values. The test with the highest GRG value is regarded as the most advantageous option among all the conducted tests.

4. Results and discussion

In this study, we explored how various machining parameters impact the tensile strength and surface roughness of a 3D-printed component. Typically, higher tensile strength and lower surface roughness were considered desirable. To achieve this, we first normalized the experimental results (table 3) on a scale from zero to one using equation (2) and equation (3), as indicated in table 4. Subsequently, we determined deviational sequences for all quality characteristics in each experimental run. Next, we calculated the grey relational coefficients (GRC) using equation (6) and presented the GRC results in table 4.

In the following step, we utilized the principal component analysis method to assess the relative importance of each performance characteristic, as per equation (8). Following the PCA, the weights assigned to tensile strength and surface roughness were found to be 0.4998 each. This indicates that within the investigated range of input parameters, both attributes carry equal significance.

Ultimately, the calculation of grey relational grades (GRG) involved the averaging of GRC values derived from the corresponding process response, as determined by equation (10). Assessment of multiple quality characteristics relied on the GRG, with a preference for higher GRG values among the experimental runs. The GRG values were graphed for different trials (see figure 2), revealing that the experiment numbered 21 recorded the highest GRG value. Therefore, the best combination of process parameters is identified with a printing speed of 100mm.s^{-1}, layer thickness of 0.1mm, and C-deposition of 15mg.

4.1. Confirmation test

Once the optimal machining parameters have been determined, the subsequent phase involves confirming the enhancement of performance characteristics through the utilization of this optimal combination. The calculation of the estimated grey relational grade using the optimal levels of these parameters is as follows:

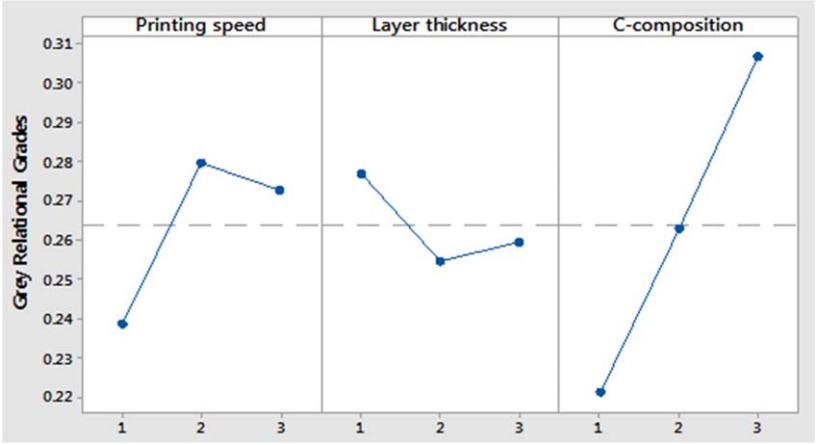

Figure 2. GRG values plot for the various experimental trials.

Table 5. Results of machining performance using initial and optimal machining parameters.

	Initial machining parameters	Optimal machining parameters	
		Prediction	Experiment
Setting Level	$A_1B_1C_2$	$A_3B_1C_3$	$A_3B_1C_3$
Tensile strength (MPa)	7.68	10.05	11.54
Surface roughness R_a(μm)	0.006	0.004	0.003
Grey relational grade	0.217	0.500	0.653

$$\hat{\gamma} = \gamma_m + \sum_{i=0}^{o} (\overline{\gamma}_j - \gamma_m) \tag{11}$$

Here, γ_m represents the overall mean of the grey relational grade, $\overline{\gamma}_j$ denotes the mean of the grey relational grade at the optimal level, and 'o' represents the number of machining parameters significantly influencing multiple performance characteristics.

The results of the confirmation experiment employing the optimal machining parameters are presented in table 5. The confirmation experiment yielded response values, with tensile strength = 10.05MPa and surface roughness = 0.004 microns. The tensile strength shows an increased value of 10.05MPa to 11.54Mpa and the Surface roughness R_a shows a reduced value of 0.004μm to 0.003μm. This study unequivocally demonstrates significant enhancements in various performance attributes within the 3D printing process.

4.2. Input-output in process parameter relationship model

Response Surface Methodology (RSM) was utilized to create a mathematical link between various input variables and outcomes. A quadratic model (a second-order polynomial equation) was developed to investigate the impacts of these variables on the overall assessment value. Employing MINITAB 17, the model coefficients were evaluated through the least square method. Equation (11) represents the anticipated quadratic model for predicting the hybrid methods mentioned earlier within the experimental region.

Equation (11) depicts the quadratic representation of the hybrid GRA-PCA model in the following manner:

Grey relational grades = 0.085 + 0.1081 Printing speed + 0.0050 Layer thickness
+ 0.0209 C-deposition − 0.0238 Printing speed*Printing speed
+ 0.0136 Layer thickness*Layer thickness
+ 0.0010 C-deposition*C-deposition
− 0.0205 Printing speed*Layer thickness
+ 0.0226 Printing speed*C-deposition
− 0.0136 Layer thickness*C-deposition

To evaluate how well the multivariate approach worked, a residual analysis was carried out to verify the suitability of the model. This analysis serves as an essential diagnostic tool to evaluate model performance. Figure 3 illustrates the results of the analysis, involving various graphical representations, such as a normal probability plot depicting standardized residuals, a scatter plot illustrating standardized residuals against the

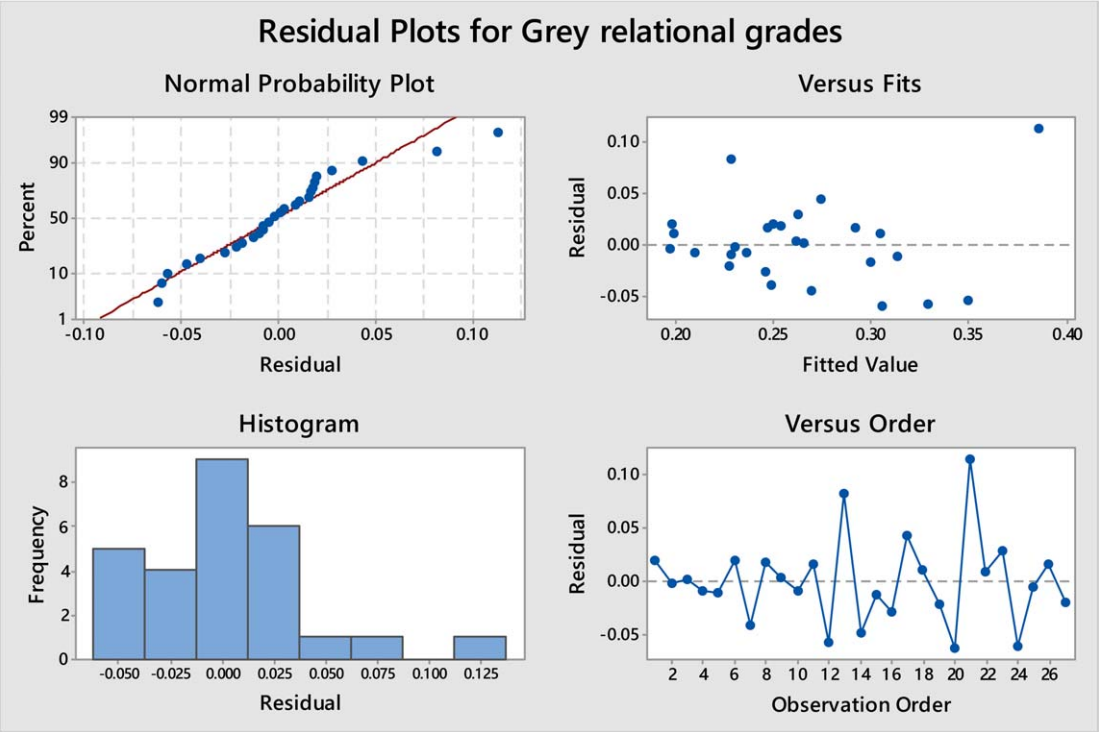

Figure 3. Residual plots for overall assessment value for suggested GRA-PCA technique.

order of observations and their corresponding fitted values, and a histogram. The absence of outliers and adherence to a normal distribution in these plots indicate the fitness of the proposed model. Furthermore, there is no discernible pattern or structure in the standardized residuals and observation orders, which serves to affirm the effective performance of the suggested model.

5. Conclusions

In this study, an innovative approach was developed to improve the mechanical performance and surface quality of parts produced using fused deposition modeling (FDM) technology. The research successfully achieved its objective by determining the most effective set of processing parameters for FDM through a hybrid multi-objective method, combining grey relational analysis (GRA) with principal component analysis (PCA). The study revealed that GRA and PCA offer a reliable approach to addressing multi-attribute optimization problems. The experimental findings indicate that carbon deposition (C-deposition) has the most significant influence on surface roughness, followed by layer thickness and printing speed. Similarly, when it comes to tensile strength, printing speed is the most influential factor, followed by C-deposition and layer thickness. Significantly, the experimental trial demonstrated the highest grey relational grade, suggesting that the optimal process parameters were achieved at a printing speed of 100mm.s^{-1}, layer thickness of 0.1mm, and C-deposition of 15mg respectively.

The implications of these findings extend to various industries and applications utilizing FDM 3D printing, promising stronger and more durable end products. Future research can explore the application of different hybrid optimization methods to further enhance the qualities of FDM-printed components. In addition, investigations should focus on characterizing surface hardness, residual stress, and microstructure.

Data availability statement

All data that support the findings of this study are included within the article (and any supplementary files).

Funding

Not applicable

Conflicts of interest/Competing interests

The authors declare that there is no conflict of interest.

Availability of data and material

All data that support the findings of this study are included within the article (and any supplementary files).

Authors' contributions

Rajeev Ranjan: Conceptualization, writing -review & editing, **Abhijit Saha:** Methodology & visualization.

ORCID iDs

Rajeev Ranjan https://orcid.org/0000-0003-1294-4765
Abhijit Saha https://orcid.org/0000-0001-9995-6288

References

[1] Thompson M S 2022 Current status and future roles of additives in 3D printing—a perspective *J. Vinyl Add. Tech.* **28** 3–16
[2] Bahnini I, Rivette M, Rechia A, Siadat A and Elmesbahi A 2018 Additive manufacturing technology: the status, applications, and prospects *Int. J. Adv. Manuf. Technol.* **97** 147–61
[3] Parandoush P and Lin D 2017 A review on additive manufacturing of polymer-fiber composites *Compos. Struct.* **182** 36–53
[4] Ranjan R, Kumar D, Kundu M and Chandra Moi S 2022 A critical review on classification of materials used in 3D printing process *Mater. Today Proc.* **61** 43–9
[5] Odera R S and Idumah C I 2023 Novel advancements in additive manufacturing of PLA: a review *Polymer Engineering & Science* **63** 3189–208
[6] Kim H, Fernando T, Li M, Lin Y and Tseng T-L B 2017 Fabrication and characterization of 3D printed BaTiO3/PVDF nanocomposites *J. Compos. Mater.* **52** 197–206
[7] Shanmugam V, Pavan M V, Babu K and Karnan B 2021 Fused deposition modeling based polymeric materials and their performance: a review *Polym. Compos.* **42** 5656–77
[8] Der Klift F V, Koga Y, Todoroki A, Ueda M, Hirano Y and Matsuzaki R 2016 3D Printing of continuous carbon fibre reinforced thermo-plastic (CFRTP) tensile test specimens *Open Journal of Composite Materials* **06** 18–27
[9] Matsuzaki R, Ueda M, Namiki M, Jeong T-K, Asahara H, Horiguchi K, Nakamura T, Todoroki A and Hirano Y 2016 Three-dimensional printing of continuous-fiber composites by in-nozzle impregnation *Sci. Rep.* **6** 1–7
[10] Hao W, Liu Y, Zhou H, Chen H and Fang D 2018 Preparation and characterization of 3D printed continuous carbon fiber reinforced thermosetting composites *Polym. Test.* **65** 29–34
[11] Monticeli F M, Neves R M, Ornaghi H L and Almeida J H S 2021 A systematic review on high-performance fiber-reinforced 3D printed thermoset composites *Polym. Compos.* **42** 3702–15
[12] Sood A K, Ohdar R K and Mahapatra S S 2010 Parametric appraisal of mechanical property of fused deposition modelling processed parts *Mater. Des.* **31** 287–95
[13] Durgun I and Ertan R 2014 Experimental investigation of FDM process for improvement of mechanical properties and production cost *Rapid Prototyping Journal* **20** 228–35
[14] Onwubolu G C and Rayegani F 2014 Characterization and optimization of mechanical properties of ABS parts manufactured by the fused deposition modelling process *International Journal of Manufacturing Engineering* **2014** 1–13
[15] Nuñez P J, Rivas A, García-Plaza E, Beamud E and Sanz-Lobera A 2015 Dimensional and surface texture characterization in fused deposition modelling (FDM) with ABS plus *Procedia Engineering* **132** 856–63
[16] Baich L, Manogharan G and Marie H 2015 Study of infill print design on production cost-time of 3D printed ABS parts *International Journal of Rapid Manufacturing* **5** 308
[17] Wu W, Geng P, Li G, Zhao D, Zhang H and Zhao J 2015 Influence of layer thickness and raster angle on the mechanical properties of 3D-printed PEEK and a comparative mechanical study between PEEK and ABS *Materials* **8** 5834–46
[18] Behzadnasab M and Yousefi A A 2016 Effects of 3D printer nozzle head temperature on the physical and mechanical properties of PLA based product *In12th international seminar on polymer science and technology* 2–5
[19] Christiyan K G J, Chandrasekhar U and Venkateswarlu K 2016 A study on the influence of process parameters on the mechanical properties of 3D printed ABS composite *IOP Conference Series: Materials Science and Engineering* **114** 012109
[20] Dawoud M, Taha I and Ebeid S J 2016 Mechanical behaviour of ABS: an experimental study using FDM and injection moulding techniques *J. Manuf. Processes* **21** 39–45
[21] Chacón J M, Caminero M A, García-Plaza E and Núñez P J 2017 Additive manufacturing of PLA structures using fused deposition modelling: effect of process parameters on mechanical properties and their optimal selection *Mater. Des.* **124** 143–57
[22] Deng X, Zeng Z, Peng B, Yan S and Ke W 2018 Mechanical properties optimization of poly-ether-ether-ketone via fused deposition modeling *Materials* **11** 216
[23] Khatwani J and Srivastava V 2018 Effect of process parameters on mechanical properties of solidified pla parts fabricated by 3D printing process *3D Printing and Additive Manufacturing Technologies* 95–104
[24] Yadav D, Chhabra D, Kumar Garg R, Ahlawat A and Phogat A 2020 Optimization of FDM 3D printing process parameters for multi-material using artificial neural network *Mater. Today Proc.* **21** 1583–91
[25] Selvam A, Mayilswamy S and Whenish R 2020 Strength Improvement of additive manufacturing components by reinforcing carbon fiber and by employing bioinspired interlock sutures *J. Vinyl Add. Tech.* **26** 511–23

[26] Kafshgar A R, Rostami S, Aliha M and Berto F 2021 Optimization of properties for 3D printed PLA material using taguchi, ANOVA and multi-objective methodologies *Procedia Structural Integrity* **34** 71–7
[27] Choudhary N, Sharma V and Kumar P 2021 Reinforcement of polylactic acid with bioceramics (alumina and YSZ composites) and their thermomechanical and physical properties for biomedical application *J. Vinyl Add. Tech.* **27** 612–25
[28] Xu C, Cheng K, Liu Y, Wang R, Jiang X, Dong X and Xu X 2020 Effect of processing parameters on flexural properties of 3D-printed polyetherketoneketone using fused deposition modeling *Polymer Engineering & Science* **61** 465–76
[29] Mani M, Karthikeyan A G, Kalaiselvan K, Muthusamy P and Muruganandhan P 2022 Optimization of FDM 3-D printer process parameters for surface roughness and mechanical properties using PLA material *Mater. Today Proc.* **66** 1926–31
[30] Heidari-Rarani M, Ezati N, Sadeghi P and Badrossamay M 2020 Optimization of FDM process parameters for tensile properties of polylactic acid specimens using Taguchi design of experiment method *J. Thermoplast. Compos. Mater.* **35** 2435–52
[31] Raju R, M.K. Varma M M and Kumar Baghel P 2022 Optimization of process parameters for 3D printing process using Taguchi based grey approach *Mater. Today Proc.* **68** 1515–20
[32] Maguluri N, Suresh G and Rao K V 2021 Assessing the effect of FDM processing parameters on mechanical properties of PLA parts using taguchi method *Journal of Thermoplastic Composite Materials* **36** 1472–88
[33] Nagarjun J, Kanchana J, Rajeshkumar G and Anto Dilip A 2023 Enhanced mechanical characteristics of polylactic acid/tamarind kernel filler green composite filament for 3D printing *Polymer Composites* **44** 7925–40
[34] Beylergil B, Al-Nadhari A and Yildiz M 2023 Optimization of charpy-impact strength of 3D-printed carbon fiber/polyamide composites by taguchi method *Polym. Compos.* **44** 2846–59
[35] Yao B, Zhu Y, Xu Z, Wu Y, Yang L, Liu J, Shang J, Fan J, Ouyang L and Fan H S 2023 Taguchi design and optimization of the PLA/PCL composite filament with plasticizer and compatibilizer additives for optimal 3D printing *Polymer Engineering & Science* **63** 3743–61
[36] Qin Y, Qi Q, Shi P, Lou S, Scott P J and Jiang X 2023 Multi-attribute decision-making methods in additive manufacturing: the state of the art *Processes* **11** 497
[37] Mahapatra S S and Panda B N 2013 Benchmarking of rapid prototyping systems using grey relational analysis *International Journal of Services and Operations Management* **16** 460
[38] Sakthivel Murugan R and Vinodh S 2020 Parametric optimization of fused deposition modelling process using grey based taguchi and TOPSIS methods for an automotive component *Rapid Prototyping Journal* **27** 155–75
[39] Koli Y, Arora S, Ahmad S, Priya, Yuvaraj N and Khan Z A 2022 Investigations and multi-response optimization of wire arc additive manufacturing cold metal transfer process parameters for fabrication of SS308L samples *J. Mater. Eng. Perform.* **32** 2463–75
[40] Patil P, Singh D, Raykar S J and Bhamu J 2022 Multi-objective optimisation and analysis of fused deposition modelling parameters: best infill patterns *International Journal of Six Sigma and Competitive Advantage* **14** 18
[41] Yilmaz S, Gul O, Eyri B, Gamze Karsli Yilmaz N and Yilmaz T 2023 Comprehensive characterization of 3D-printed bamboo/poly (lactic acid) bio composites *Polymer Engineering & Science* **63** 2958–72
[42] Mukherjee D, Ranjan R and Moi S C 2022 Multi-response optimization of surface roughness and MRR in turning using taguchi grey relational analysis (TGRA) *International Research Journal of Multidisciplinary Scope* **03** 01–07
[43] Saha A and Majumder H 2020 Multi-attribute optimisation of submerged arc welding process parameters using taguchi GRA-PCA hybrid approach *Australian Journal of Mechanical Engineering* **20** 1207–12
[44] Ranjan R, Saha A and Kumar Das A 2022 Comparison of multi-criteria decision making methods for multi optimization of GTAC process parameters *Periodica Polytechnica Mechanical Engineering* **66** 166–74
[45] Unnikrishna Pillai J, Shunmugavel M, Thangaraj M, Goldberg M, Singh R and Littlefair G 2022 Effects of machining parameters on enhancing alpha-beta titanium alloy using taguchi-grey relational analysis for aerospace applications *Proc. Inst. Mech. Eng. Part E J. Process Mech. Eng.* **237** 118–27
[46] Saha A and Mondal S C 2016 Multi-objective optimization in WEDM process of nanostructured hardfacing materials through hybrid techniques *Measurement* **94** 46–59